NSUK Journal of Science & Technology, Vol. 7(1): pp. 50-58, 2020 Print: ISSN: 2756-696X
On-line: ISSN 2756-6951
Website: www.nsukjst.org.ng

SYNTHESIS AND CHARACTERIZATION OF ALUMINUM DOPED ZINC OXIDE AS A TRANSPARENT CONDUCTING MATERIAL FOR OPTOELECTRONICS APPLICATIONS

Bilya, M. A., Sarki, M. U. and Wakili, B.

Nasarawa State University, Keffi, Faculty of Natural and Applied Sciences, Department of Physics,
P.M.B. 1022, Keffi, Nasarawa State, Nigeria.
musabilya@nsuk.edu.ng, musarki@nsuk.edu.ng, wbilyaminu@gmail.com

ABSTRACT

Aluminum doped Zinc Oxide thin film was obtained at 0%, 4%, 7%, 10% and 13% doping levels using aerosol assisted chemical vapour deposition technique to yield high quality thin films. The Optical characterization was done using UV-VIS 700 Spectrophotometer (Malvern Panalytical) whereby the transmittance, absorbance and reflectance of the thin films were determined. The electrical properties which include resistivity and conductivity were obtained using a four point probe technique, and the energy band gap was also calculated. It was found that the transmittance over the visible range decreases with decreased Aluminum doping concentration. Hence, the un-doped ZnO sample was found to produce high transmittance as compared to the doped samples. The Aluminum doped Zinc oxide thin films (Al:ZnO) were found exhibiting low absorbance within the visible region (400-1100nm). But there was a significant increase in absorbance as the aluminum doping increases, which subsequently decreases the transmittance. The reflectance was found to increase with increased doping level and the refractive index calculated is 2.4. The increased doping levels of Aluminum decreases resistivity, but increases the conductivity. Aluminum co-doped Zinc Oxide (Al:ZnO) was found to cause decrease in the energy band gap (Figure 9) which plays an important role in electrode applications such as the dye-sensitized solar cells and the piezoelectric nanogenerators. The decreased Energy Band Gap influences the electron excitation energy from the valence band to the conduction band for possible photovoltaic applications.

Keywords**:** *Transmittance, Nanogenerators , Doping, Spectrophotometer, Absorbance, Conductivity*.

INTRODUCTION

The range of its electrical and optical properties, high chemical and mechanical stabilities makes Aluminum doped zinc oxide (AZO) thin films technologically important and suitable for variety of applications. Some of these applications range from the surface acoustic devices because of the AZO thin films large piezoelectric constants, to the solar cells since their optical band gap (3.3eV) is wide enough to transmit most of the useful solar radiation ((Mugwang'a et al., 2015).

These films can be used as surface acoustic wave devices, because of their large piezoelectric constant, and also solar cells, since their optical band gap (3.3eV) is wide enough to transmit most of the useful solar radiation (Mugwang'a et al., 2015)

The rise in the global energy demand and the international recognition of global warming are stimulating tremendous industrial and academic efforts to replacing fossil fuels with other alternative energy sources which are perceived more economically, politically and environmentally favorable. Fossil fuels are being consumed at extremely large amounts and it is estimated that resources will start to run out in the next 50 years (Minami, 2005). Transparent conductive oxides (TCO's) seem to be a contradiction. Most conducting materials are not transparent, and most transparent materials are not conductive. TCO's are a kind of materials possessing these two properties, generally mutually exclusive. To achieve this combination, a high concentration of carriers wide band gap and enough mobility are required.

Transparent conducting thin films (TCO) have great significance in the optical and electrical devices, i.e., dye-sensitized solar cells and photovoltaic flat panel displays. Usually thing films are made up of semiconducting metal oxide with a trivalent or pentavalent doping elements for the development of high electrical conductivity (Chopra, 1983). At the beginning of the twentieth century, Badeker (1907) developed good electrically conductive transparent cadmium oxide thin film via sputtering and thermal oxidation of cadmium on glass substrate. Indium-doped tin oxide, indium oxide and zinc oxide transparent conducting films were established from the last three decades. However, their performances were limited to solar cells due to their low mobility of charge carriers and high electrical resistivity (Coutts *et al.*, 1996).

Thin films made of Indium-doped tin oxide (ITO) have good electrical conductivity and are highly transparent. However, indium is inadequate element on earth, owing to its growing cost of fabrication, as well as its toxic nature which is dangerous to human health and environment. Due to this reason, new TCO combinations were needed to give the optimum transparent and optical properties for the organic electronic devices. Nowadays, the interest is shifted to the ZnO films in which electrical and transparent properties can be altered by doping the groups III and VII elements (Shelake et al., 2008). The ZnO thin films have considerable optical transparency, electrical conductivity, low cost, non-toxicity and have good stability to plasma environment. However, the semi conductive properties of Zinc Oxide thin films could not compete with the performance efficiency of ITO films. The conductivity of ZnO thin film could be improved by optimizing the doping levels and processing parameters. By doing this, ZnO thin films will be better alternative towards replacing ITO for other promising applications which may include solar cells, transducers, gas sensors and heating mirrors (Kim & Tai, 2007; Wu, 2010).

In the previous decade, the extrinsic zinc oxide (ZnO) based thin films doped with different elements, i.e. manganese (Mn), gallium (Ga), aluminum (Al), indium (In) and tin (Sn) have been developed (Hao, 2002; Lee & Park, 2003; Chen *et al.,* 2007). Beside other doping elements, the change in atomic concentration of Al in ZnO can influence the film thickness and crystallite size (Lee & Park, 2003). The resistivity of intrinsic ZnO thin films can be decreased by doping Al up to 1 at % (Salam, 2003).

Different methods of ZnO depositions on glass have been adopted for example, the sol–gel process, plasma jet (Hsu, 2011)); spray pyrolysis, (Sahay & Nath, 2008) magnetron sputtering (Ruske, 2008; Wu, 2010) thermal degradation of hydrogels (Tredici, 2011) and chemical vapor deposition (Polley, 1996). Additionally, sputtering is the widely used method for ZnO thin film deposition towards achieving good optical and electrical properties at low temperature. However, this method is expensive and has low deposition rate. Sol–gel method is getting much attention because of its simplicity and low cost. The Sol-gel method is capable of producing high quality coatings on both large and small size substrates, which may be employed for advanced applications (Silva et al., 1999; Lee & Park, 2003).

In Sol–gel method, some of the important factors that affect the characteristics of the conductive oxide films are pH, substrate/film interaction, chemical composition of the sol, viscosity and coating technique (dip or spin). After the deposition process, furnace atmosphere, drying and annealing time are some of the highly significant factors to be considered (Silva & Darbello, 1999).

Shan & Yu (2004) applied the pulse laser deposition technique in depositing pristine and Aluminum doped Zinc Oxide thin films at variable temperatures on glass substrate. It was observed that the energy band gap of the pristine ZnO increases and even saturates with the temperature. However, the energy band gap of the Aluminum doped zinc oxide decreases exponentially as the temperature increases.

Influence of the doping levels of Aluminum Zinc oxide thin films by depositing the films on Indium Tin Oxide substrates was observed and that the thin films exhibited an optical transmittance as high as 90% in the wavelength range 100-1000nm. The optical band gap increased from 3.33 to 3.45eV. The lowest resistivity was recorded at 4.78 x 10^{-3} Ωcm in the film doping of 3mol% Aluminum Zinc oxide concentration. Zn^{+2} in the ZnO are usually replaced with Al^{+3} ions to give the property of photoluminesces in the ultraviolet (UV) and visible spectral range because of its optical properties and excitonic emission at room temperature (Ali et al., 2015).

Thus, in this research, Aluminum doped Zinc Oxide (Al:ZnO) was fabricated as a transparent conducting material for optoelectronic applications

Literature on Crystal Structure and Chemical Bonding of ZnO

Zinc oxide is a semiconducting compound of the group-II element ^{30}Zn and the group VI element ^{8}O. Zinc has five stable isotopes, the prevalent ones are ^{64}Zn (48.89%), ^{66}Zn (27.81%), and ^{68}Zn (18.57%), while oxygen almost purely consists of the isotope ^{16}O (99.76%). Zinc has the electron configuration $(1s)^2(2s)^2(2p)^6(3s)^2(3p)^6(3d)^{10}(4s)^2$: the oxygen configuration is $(1s)^2(2s)^2(2p)^4$. The ZnO binding in its crystal lattice involves a sp^3 hybridization of the electron states, leading to four equivalent orbitals, directed in tetrahedral geometry. In the resulting semiconducting crystal, the bonding sp^3 state constitutes the valance band, while the conduction band originates from its anti-bonding counterpart. The resulting energy gap is 3.4 eV, i.e., in the UV spectral range, which has triggered interest in ZnO as a material for transparent electronics (Seshan, 2012). The cohesive energy per bond is as high as 7.52 eV, which also leads to a very high thermal stability: The melting temperature, Tm = 2,242K. For comparisons, the melting temperature of ZnS is considerably lower: Tm = 1,799K (Claus *et al*., 2010). Zinc oxide normally has the hexagonal wurtzite (Fig 1.0 b) crystal structure. Additionally, the wurtzite phase, ZnO is also known to crystallize in zinc blende (Fig 1.10 a) and cubic crystal structure. Nanoparticles formed by the oxidation of zinc vapor have the zinc blende structure when smaller than 20 nm, and form tetrapod like crystals on further growth (Shiojiri *et al*., 1981). ZnO prepared via the flash evaporation method have a cubical crystal structure (Tanigakit *et al*., 2002).

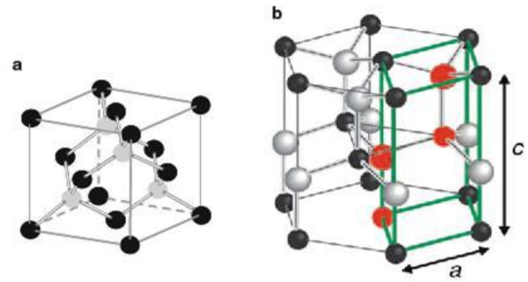

Figure 1: (a) Zinc Blender Structure (b) Wurtzite Structure (Tanigakit *et al*., 2002).

MATERIALS AND METHODS

Materials

The materials used to carry out the research work are as follows:

(i) U.V-VIS Spectrophotometer, (ii) 4 point probed (ii) Profilometer (iv) Insulin String (v) Spatula (vi) Perish dish (vii) Aluminum foil (viii) Beaker (ix) Electronic weighing balance (x) Stirring band , (xi) Magnetic stirrer (xii) 3D Printer (xiii) Aluminum zinc oxide (AlZnO) Solution (xiv) Methanol (xv) Propanol (xvi) Frosted Glass substrates (xvii) Zinc acetate (ZAD) (($Zn(CH_3COO)$ (xviii) Aluminum Chloride ($AlCl_3$).

Method

AACVD Technique

Aerosol assisted chemical vapor deposition (AACVD) is a synthesis method where the substrate is exposed to one or more in-volatile precursor, suspended in a liquid-gas aerosol (generate ultrasonically), which react or decompose on the surface to produce a deposit. Aerosol assisted chemical vapor deposition (AACVD) involves the formation of a thin solid film on a substrate via chemical reactions of precursors in the vapor phase. It is the chemical reaction, which distinguishes CVD from physical vapour deposition (PVD), processes (Choy, 2003). The chemical reactions occur homogeneously in the gas phase and/or heterogeneously on the substrate, the latter is desired in order to obtain high quality films (Jone, 2009). CVD requires the delivery of a precursor into a gas stream, transport of the precursor to a substrate and the application of energy to cause a reaction. The key steps of CVD as itemized by Jone (2009) are:

- Evaporation and transport of reagents in the bulk gas flow region into the reactor;
- Mass transport of the reactants to the substrate surface;
- Adsorption of the reactants on the substrate surface;
- Surface diffusion to growth sites;
- Nucleation and surface chemical reactions leading to film growth;
- Desorption and mass transport of remaining fragments of the decomposition away from the reaction zone.

The substrate temperature and the pressure of the reactor as well as the complex gas-phase chemistry occurring in the reaction zone, determine the film growth rate in thermal CVD. At lower substrate temperatures, the film growth rate is determine by the kinetics of the chemical reactions occurring either in the gas phase or on the substrate surface, this is generally denoted as surface reaction limited film growth. As the temperature is increased, the film growth rate becomes almost independent of temperature and the growth is determined by the mass transport of the precursors through the boundary layer to the growth surface. This is known as the mass transport limited film growth.

Precursor solution

All The chemical system used involves a precursor for Zn: Zinc acetate Zn (CH_3COO) of 1.09g and for Al: Aluminum chloride ($AlCl_3$) of 0.67g. Zinc acetate Zn(CH_3COO) were dissolved in 50ml of a solution of propanol (C_3H_8O) (solvent) and Aluminum chloride ($AlCl_3$) were dissolved in 50ml of a solution of methanol (CH_3OH) which serve as stabilizer for the mixture. The solution was then stirred at normal room temperature until a clear and homogeneous solution is obtained. The percentage Al doped ZnO sample each was poured into a separate beaker of which is now ready for the deposition.

The table 1 below shows the variation of the Al percentage doped into Zno

Deposition using 3D - Printer

The 3D Printer machine is fixed to power supply, which then undergo automatic and manual calibration (set to work on AACVD mode). A cleaned substrate was fixed in the substrate holder and the nozzle is set directly at the substrate surface of which the distance between the nozzle and the substrate is 6mm. In addition, the target region of the substrate will be set to Y-axis and X-axis respectively, and then a 1ml string is used to fetch each sample from its beaker into a 1 ml string attached to the nozzle of the 3D-printer. The mode of deposition onto the substrate is Rastering mode. In this research, 0.2ml was deposited twice on each substrate (0.4ml) of which the time interval for depositing 0.4ml is two (2) minutes and the deposition temperature is 260^{o}C per sample.

The experimental set-up used to carry out the research is as shown in Figure 2.

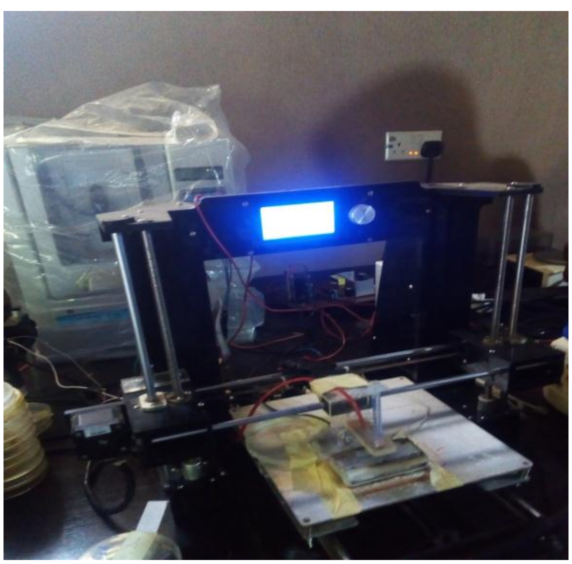

Figure 2: Experimental set-up for AACVD

RESULTS

Thin Film Thickness

Thin film thickness of AZO determined using a profilometer for the different percentages of Aluminum dopants are presented in table 2.

Optical Characterization

Transmittance (T): is the amount of transmitted radiation over the incident power. All samples have an average transmittance in visible region of above (60%) from the computed result. The transmittance above (60%) is obtained, because ZnO is a semiconductor with a wide direct band gap of 3.3 eV. It was observed, that the transmittance over the visible range decreases as the concentration of Aluminum increases. This agrees very well with Elim et al., who reported significantly reduced transmission when ZnO was doped with higher percentage of aluminum; hence the un-doped sample produces high transmittance as compared to the 4%, 7%, 10% and 13% doped. Due to the high transmittance, these films have good optical properties for solar cells window applications.

Figure 3 illustrates the transmittance of the thin film against the Al percentage dopant.

Absorbance of Al:ZnO thin film

Absorption (A) is the amount of absorbed radiation over the amount of incoming radiation power. Figure 6.22 below, illustrates the optical absorption spectra of Al-doped ZnO thin films for various Al concentrations. The absorption spectra revealed that all Al:ZnO films exhibit low absorbance in the visible region (from 400-1100nm) especially for the un-doped , 4% and 7% for the doped sample. The graph below signified the increase in absorbance as the Al concentration is increased, which also decreases the transmittance level.

The following figures represent individual absorption spectra per sample of Al:ZnO thin film:

Reflectance of the material

Reflectance (R): Reflectance is the amount of reflected radiation over the amount of incoming radiation power. Equation (6.1) below is used to obtain the value of reflectance of the material. The obtained results are as tabulated below and the refractive index of the material is given as thus:

$$R + T + A = 1 \qquad (1)$$

From the above graph, the value of the reflectance increases as Al impurity was added to the ZnO, therefore subsequently decreasing the transmittance and increases the absorbance. The refractive index of the material calculated is:

Refractive index of the material = 2.4

Electrical Properties

Resistivity of Al:ZnO Thin Film

The resistivity of the Al:ZnO thin films were measured using a four point probe and the results are presented in Table 5.

The resistivity result of Al:ZnO film is as shown in Figure 7. It decreases as a small amount of 13% Al doping takes place, as compared to the un-doped sample. However, the 4%, 7% and 10% doped increases due to the thickness of the thin film. Mainly, the increase doping levels of impurity usually decrease the resistivity and increase the conductivity of the sample. The optimum Al doping level was found at 13 % in Al:ZnO film.

Conductivity of Al:ZnO Thin Films

The conductivities of these samples were computed from the results of the resistivity values in table 5, the following equations were used for this computation, and the conductivity of each sample are presented in the following table:

$$\alpha \propto (hv - Eg) \quad (2)$$

$$\mathrm{E} = \frac{hv}{\lambda} \quad (3)$$

Energy Band Gap

Energy band gap of the thin film is determined using equation (2) and the results are presented in the Table 7.

From figure 9, the value of the band gap obtained decreases with small amount of increase in the impurity (Al dopant). The decreased band gap energy in ZnO structure plays an importance role in electrode applications, such as the dye-sensitized solar cell and piezoelectric nanogenerator. The band gap energy influences the excitation energy of electron, from valence band to the conduction band.

DISCUSSION

All the samples obtained revealed a low absorbance, hence having an average transmittance above 60% in the visible range, which is less than the one reported by Alaeddine et al. (2009). The un-doped samples have a greater transmittance of 86% as compared to the 4%, 7%, 10%, and 13% doped samples. The effect of Al doping can be clearly seen on the transmittance of the films. The transmittance spectra films were declined for the increased doping of Al, which quite agrees well with Shelake et al. (2018). This signifies that an increase in the impurity level subsequently lead to the decrease in transmittance level (Fig.3a) which agrees well with the study of Alaeddine et al. (2009). The resistivity calculated are 37.20Ωm, 37.49Ωm, 66.01Ωm, 41.44Ωm and 35.13Ωm. While the conductivity calculated, are $2.68\times10\Omega^{-1}m^{-1}$, $2.66\times10\Omega^{-1}m^{-1}$, $1.51\times10\Omega^{-1}m^{-1}$, $2.40\times10\Omega^{-1}m^{-1}$, $2.84\times10\Omega^{-1}m^{-1}$. Low resistivity of 35.13Ωm was recorded at 13% doping, which equally yields the highest conductivity of $2.84\times10\Omega^{-1}m^{-1}$ among the samples. This shows that a material with a low resistivity is highly conductive. This increase in conductivity is brought by the aluminum doping, whereby the concentration of the free charge carriers in ZnO increases by the aluminum doping because aluminum has one valence electron more than zinc. Thus, it has been shown that aluminum doping enhances the electrical conductivity and optical transmittance of ZnO films (Alaeddine et al., 2009). The thicknesses of the samples measured using a Profilometer are: 0.950µm, 0.972µm, 1.174µm, 1.110µm and 0.956µm respectively.

CONCLUSION

In conclusion, the AZO thin film obtained using aerosol assisted chemical vapour deposition yield a quality thin film, having low absorbance all through and transmittance above 60% in the visible range per sample. Due to the high transmittance of the thin film, these films have good optical properties for photovoltaic solar cells applications. It was observed that the transmittance over the visible range decreases as the concentration of Aluminum increases. This agrees very well with Elim et al. (2000). As the transmittance became higher, the electrical resistivity decreases. Films doped with 13% Al had low resistivity of 35.13Ωm and high conductivity of $2.84\times10^{-2}\Omega^{-1}m^{-1}$ with the thickness of 0.956µm. Thus, by doping ZnO with Al at %, we can optimize and improve the transmittance and conductivity, lower the absorption, resistivity and the band gap energy of Al doped ZnO films and explore the AZO potential in photovoltaic energy applications and light emitting devices.

RECOMMENDATION

- Post deposition treatment such as annealing should be investigated in order to enhance the structural, optical and electrical properties of Aluminium zinc oxide (Al:ZnO)
- Other deposition parameters such as concentration of the precursor, substrate temperature and the used of polymer substrate should be investigated in order to enhance the conductivity, crystallinity and homogeneity of the film.
- The structural properties should be investigated using X-ray Diffractormeter (XRD) because it is faster and cheaper.

REFERENCES

Alaeddine, A., Rachidi, I., Bahsoun, F., Mohanna, Y., Bazzi, O and Hassa, F.E.H. (2009). Influence of Al dopant on the optical and electrical properties of Zinc Oxide Thin Films prepared by Spray Pyrolysis. *Journal of Applied Sciences*, 9(8): 1588-152.

Babu, V. S. (2009). Solid state Device and Technology (3rd Ed.). Pearson. India. pp. 30-35.

Badeker, K. (1907). Electrical conductivity and thermo-electromotive force of some metallic compounds. Ann Phys, 22(6): 749–766.

Balandin, A.A. & Wang, K.L. (2006). *Handbook of semiconductor Nanostructures and Nanodevice* (Vol.5). American Scientific Publishers. pp. 21-23.

Brown, M and Jakeman, F. (1996). Theory of four point probe technique as applied to film layers on conducting substrates. *Brit J appl Phys*., 17(5): 1146 - 1149.

Busch, G. (2003). Early history of the physics and chemistry of semiconductors-form doubts to fact in a hundred years. *European Journal of Physics*, 10(4), 254-264.

Callister, W.D. & Rethwisch, D.G. (2007). *Materials Science and Engineering: An Introduction*, Vol. 7. Wiley, New York. pp. 205-210.

Chen, W. & Wang, M. (2007). Influence of doping concentration on the properties of ZnO: Mn thin films by sol–gel method. *Elsevier*, 81(7):894–898

Chen, Z. (2013). Fabrication of highly transparent and conducting indium-tin oxide thin films with a high figure of merit via solution processing. *Langmuir*, 29(45): 13836-13842.

Chopra, K.L. (1983). Transparent conductors a status review. *Thin Solid Films*, 102(1):1–46.

Choy, K. L. (2003). Chemical vapour deposition of coatings. *Material Science*, 23(2): 4-9.

Dhakal, T. (2012). Transmittance from visible to mid infra-red in AZO films grown by atomic layer deposition system. *Solar Energy*, 86(10):1306-1312.

Djouadi, D. (2012). Amplification of the UV emission of ZnO: Al thin films prepared by sol gel method. *Journal of Material Environmental Science*, 3(3):585–590.

Gupta, N., Alapatt, G.F., Podila, R., Singh, R. and Poole, K.F. (2009). Prospects of nanostructured-base solar cell for manufacturing future generation of photovoltaic modules. International *Journal of Photoenergy*, 10(4): 1155-1159.

Hao, X. (2002). thickness dependence of structural, optical and electrical properties of ZnO: Al films prepared on flexible substrates. *Applied Surface Science*, 189(2):18–23.

Hayamizu, S. (2011). Principle of thin film deposition. *Applied Physics*, 8(4): 90-96.

Hecht, D. S. & Hu, I. G. (2011). Emerging Transparent Electrodes Based on Thin Films of Carbon Nanotubes, Graphene and Metallic Nanostructures. *Advanced Materials*, 23(10): 1482–1513.

Hernandezbattez, A., Gonzalez, R., Viesca, J., Fernandez, J., Diazfernandez, J., Machado, A.,Chou, R. and Riba, J. (2008). CuO, ZrO_2 and ZnO nanoparticle as

antiwear additive in oil lubricant. *Wear*, 265 (4): 422-428.
Hook, J. R. and Hall, H. E (2011). Solid state Physics. John Wiley & sons. pp. 111-115.
Hsu, Y.W. (2011). Deposition of zinc oxide thin films by an atmospheric pressure plasma jet. *Thin Solid Films*, 519(10):3095–3099.
Jang, K., Park, H., Jung, S., Duy, N.V. and Kim, Y. (2010). Optical and electrical properties of thin film. *Journal of Material Science*, 56(11): 3232-3236.
Khan, Z. R. (2011). Optical and structural properties of ZnO thin films fabricated by sol–gel method. *Mater Sci. Appl.*, 2(5):340–345.
Kim, Y.S and, Tai, W.P. (2010). Electrical and optical properties of Al-doped ZnO thin films by sol–gel process. *Applied Surface Science*, 253(11):4911–4916.
Korotchenkov, G. (2013). *Thin metal films. Handbook of Gas Sensor Materials. Integrated Analytical Systems.* Springer. pp. 153–166.
Lee, J.H.and Park, B.O. (2003). Transparent conducting ZnO: Al, In and Sn thin films deposited by the sol–gel method. *Thin Solid Films*, 426(1):94–99
Marcel, D. L. (2006). Zinc oxide (zinc white): pigments, inorganic chemistry, Wiley-VCH, Weinhem. *Materials Science*, 48(2):57–170
Mattox, D.M. (2003). *The Foundations of Vacuum Coating Technology*. Norwich: Noyes. William Andrew Publishing. pp.208-216.
Mkawi, E.M., Ibrahim, K., Ali, M.K.M., Farruku, M.A. & Mohamed A.S. (2015). The Effect of Dopant concentration on Properties of Transparent Conducting AL-doped ZnO Thin Films for Efficient Cu_2ZnSnS_4 Thin Film Solar Cells Prepared by Electrodeposition Method. *Applied Nanoscience*. 5: 993 – 4984.
Mugwang'a F. K., Karimi, P. K., Njoroge, W. K. and Omayio, O. (2015). Characterization of Aluminum doped ZnO (AZO) thin films prepared by reactive thermal evaporation for solar cell applications. *J. Fundamentals of Renewabale Energy and Applications* 5170. Doi10.4172/20904541.1000170
Nelson, J. (2011). *The physics of solar cell*. London: imperial college press. pp.245-254
Ng, Z. N. (2012). Effects of annealing temperature on ZnO and AZO films prepared by sol–gel technique. *Applied Surface Science*, 258(24):9604–9609
Ohring, M. (2001). *Materials Science of Thin Films* (2nd ed.). Boston: Academic Press. pp. 35-39
Ouyang, J., Chu, C. W., Chen, F. C., Xu, Q. and Yang, Y. (2005). High conductivity poly (3,4-ethylenedioxythiophene) poly (Styrene sulfonate) Film and its Application in polymer optoelectronic Device. *Advance Functional Material*, 15(2): 203-208
Phillip, J. M. (1994). Transparent conducting thin-film of GaInO3. *Applied physics*, 65(6):115-117.
Polley, T.A. (1999). Deposition of zinc oxide thin films by combustion CVD. *Thin Solid Films,* 357(2):132–136.
Ren, X. (2015).optically enhanced semi-transparent organic solar cells through hybrid metal/nanoparticle/dielectric nanostructure. Nano Energy, 17(9): 187-195.
Rnjdar, R. M. & Ali, A.B. (2007). *Optical properties of thin film.* Sulaimani University College of Science, Physics Department. 24 p.
Ruske, F. (2008). Reactive deposition of aluminium-doped zinc oxide thin films using high power pulsed magnetron sputtering. *Thin Solid Films.* 516(14):4472–4477.
Sahay, P. P. and Nath, R. K. (2008). Al-doped zinc oxide thin films for liquid petroleum gas (LPG) sensors. *Sens Actuator B Chem*, 133(1):222–227.
Salam, S. (2013). Sol–gel synthesis of intrinsic and aluminum-doped zinc oxide thin films as transparent conducting oxides for thin film solar cells. *Thin Solid Films*, 529(5):242–247.
Shan, F. K., and Yu, Y. S. (2004). Band Gap Energy of Pure and Al-dped ZnO Thin Films. *Journal of European Ceramic Society*, 24(6):189-1872. DOI: 10.1016/S0955-2219(OS)00490-4.
Shelake, V., Bhole, M.P., & Patil, D.S. (2008). Aluminium doped zinc oxide films as a transparent conducting electrode for organic light emitting devices. *Optoelectronics and Advanced Materials, Rapid Communications*, 2(6): 353 – 355.
Seshan, K. (2012). *Handbook of Thin Film Deposition* (3rd ed.). Amsterdam: Elsevier. pp.34-38
Shadia, J., Naseem, M. and Riyad, N. (2009). Electrical and optical properties of ZnO:Al thin film prepared by pyroysis technique. Faculty of Science; Physics Department, University of Jordan; Ammam, 11942, Jordan. pp.113-119.
Shockley, W. (1950). *Electrons and holes in semiconductors with application to transistor electronics.* R. E. Krieger Pub. Co.
Silva, R. F. and Darbello, M. E. (1999). Aluminium doped zinc oxide films: formation process and optical properties. *Journal of Nano Crystals Solids*, 247(1): 248–253.
Tam, H. (2015). The solar singularity. Greentech Media. Retrieved.
Tang, C.W. and Albrecht, A.C. (1975). Photovoltaic effects of metal-chlorophyll- a-metal sandwich cells. *Journal of Chemistry Phys*, 62(8): 21-39
Tang, W. and Cameron, D. C. (1994). Aluminum doped zinc .oxide transparent conductors deposited by the sol–gel process. *Thin Solid Films*, 238(1):83–87.
Tredici, I.G. (2011). Micropatternerned nanocrystaline zinc oxide thin films obtained through metal-loaded hydrogels. *Thin Solid Film*, 519(18): 5854-5860.
Wu, G.M., Chen, Y.F., Lu, H.C. (2011). Aluminum-doped zinc oxide thin films prepared by sol-gel and RF magnetron sputtering. *Appl Phys Pol,* 120(1):1–149.
Yacobi, B. G. (2003). *Semiconductor material: an introduction to basic Principle*, Springer, pp.1-3
Yu, P. Y. & Cardona, M. (2001). *Fundamentals of Semiconductors: Physics and Materials Properties,* (3rd ed.) Springer-Verlag.
Zhou, H.M. (2007). Preparation of aluminum doped zinc oxide films and the study of their microstructure, electrical and optical properties. *Thin Solid Films*, 515(17): 6909–6914.

Table 1: Percentage of Al doped into ZnO

S/N	Dopant Conc. (%)	Zn(ml)	AL(ml)	Al:ZnO(ml)
1	0	3	0	3
2	4	2.88	0.12	3
3	7	2.79	0.21	3
4	10	2.70	0.30	3
5	13	2.61	0.39	3

Table 2: The Al doping ratio and film thickness

Sample	Al Doping (Atomic%)	Thickness (μm)
1	0	0.950
2	4	0.927
3	7	1.174
4	10	1.110
5	13	0.956

Table 3: Transmittance of the Thin Film

S/N	Percentage of Al dopant (%)	Transmittance (%)
1	0	86.09
2	4	67.92
3	7	69.50
4	10	65.61
5	13	62.80

Table 4: Reflectance per Al dopant

S/N	Percentage of Al dopant (%)	Reflectance (%)
1	0	7.4
2	4	15.3
3	7	14.7
4	10	16.1
5	13	17.0

Table 5: Resistivity of Al:ZnO Thin Film

S/N	Percentage of Al dopant (%)	Resistivity (Ωm)
1	0	3.72×10^{-5}
2	4	3.75×10^{-5}
3	7	4.45×10^{-5}
4	10	4.14×10^{-5}
5	13	3.51×10^{-5}

Table 6: Conductivity of Al:ZnO Thin Film

S/N	Percentage of Al dopant (%)	Conductivity ($\Omega^{-1}m^{-1}$)
1	0	2.69×10^{-6}
2	4	2.67×10^{-6}
3	7	2.25×10^{-6}
4	10	2.42×10^{-6}
5	13	2.85×10^{-6}

Table 7: Energy band gap (Eg) of the thin film

S/N	Aldoping (atomic %)	Energy BandGap (Eg) (eV)
1	0	3.23
2	4	2.41
3	7	2.39
4	10	2.38
5	13	2.31

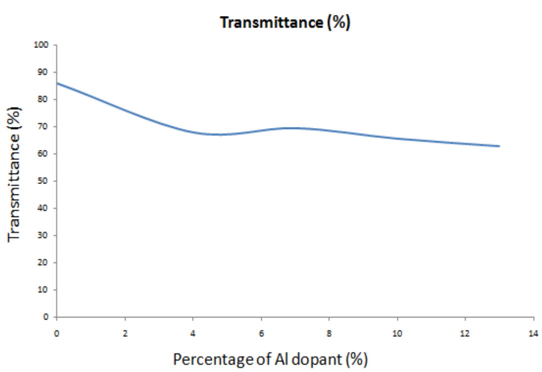

Fig 3 (a): Graph of Transmittance against Al Dopant

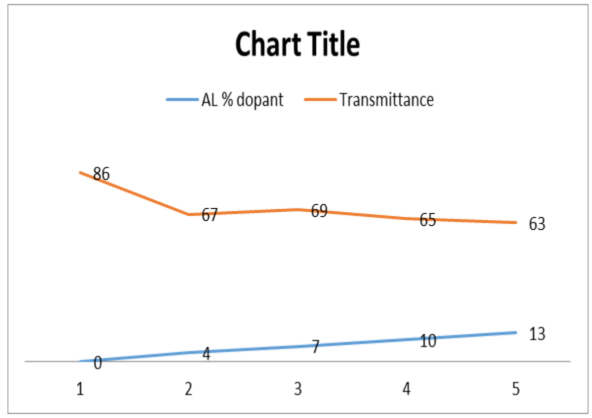

Fig. 3 (b): Graph of Percentage Chart Title

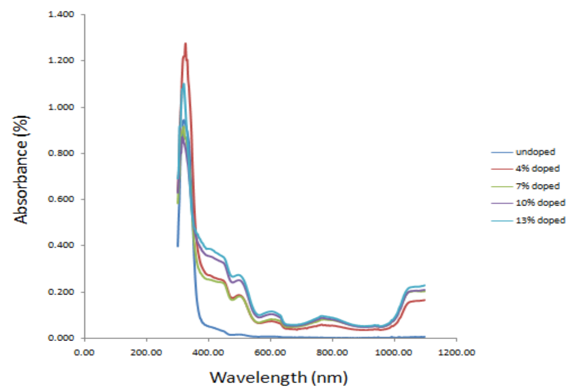

Figure 4: Graph of Absorption Spectra against Al dopant

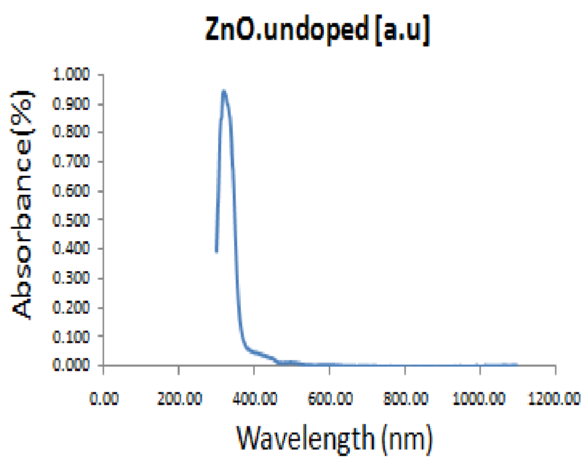

Figure 5 (a) Graph of un-doped ZnO

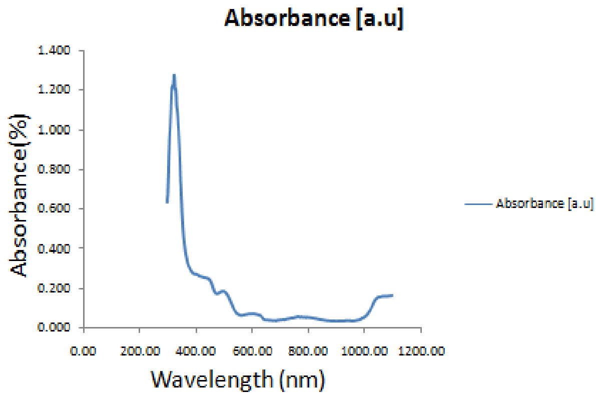

Figure 5(b) Graph of 4% doped Al:ZnO

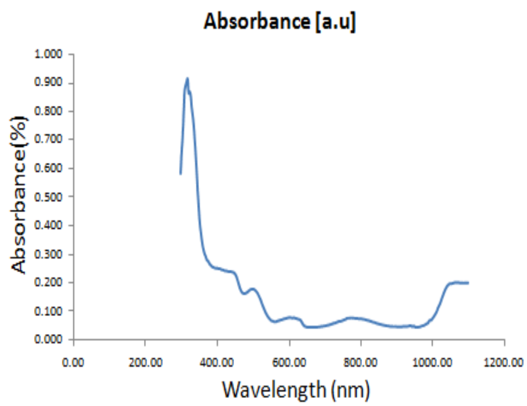

Figure 5 (c) Graph of 7% doped Al:ZnO

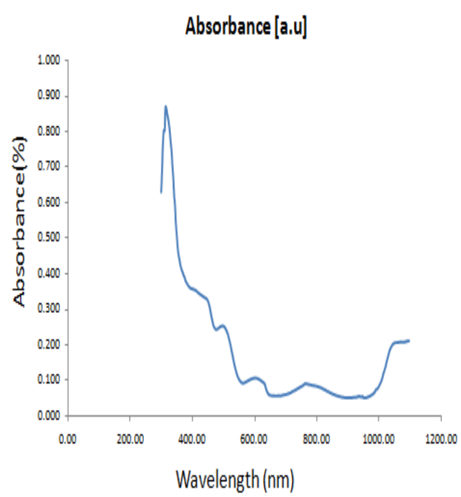

Figure 5 (d) Graph of 10% doped Al:ZnO

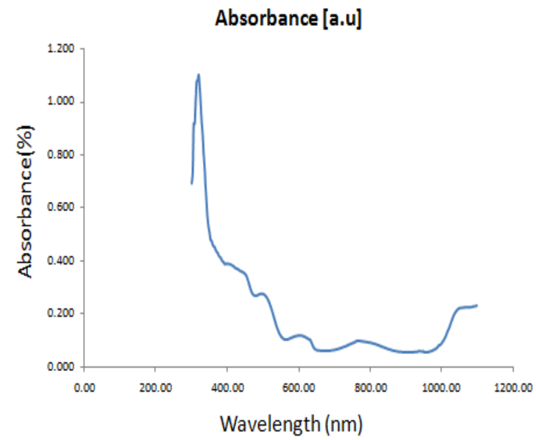

Figure 5 (e) Graph of 13% doped Al:ZnO

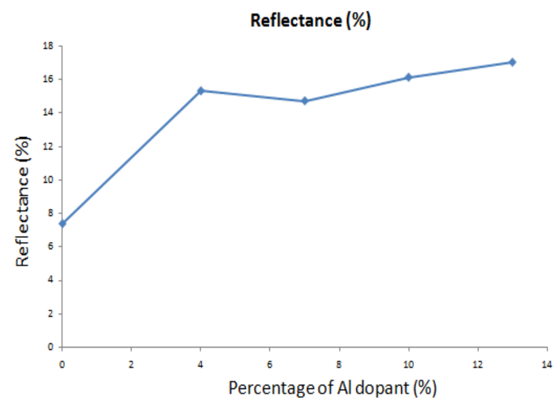

Figure 6: Graph of Reflectance against Al percentage

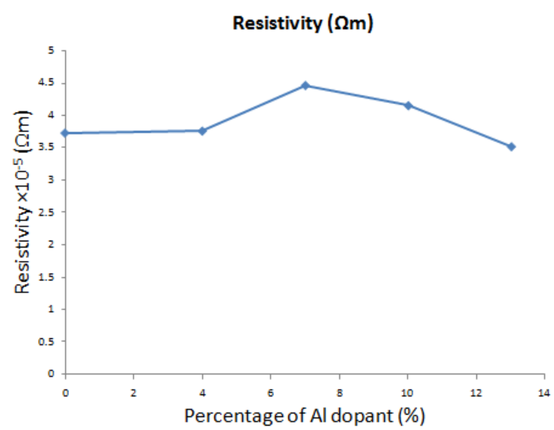

Figure 7:Graph of Aluminum Doping Levels with Sheet Resistivity

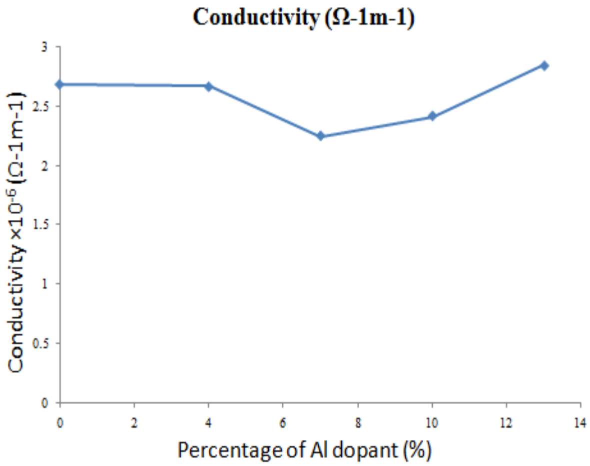

Figure 8: Graph of conductivity showing percentage Aluminum Doping Levels.

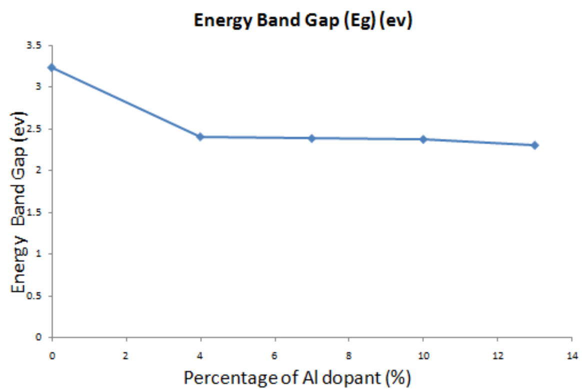

Figure 9: Graph of Aluminum Doping Levels with Band gap